GAS JET TARGETS

M. Macri
CERN, Geneva, Switzerland

ABSTRACT

The use of a molecular gas 'jet' as an internal target in a storage ring is described.

1. INTRODUCTION

The availability of intense antiproton sources from stochastic cooling has opened up new experimental possibilities in high-energy physics.

The use of gaseous internal targets in antiproton storage rings [the CERN Intersecting Storage Rings (ISR), the Super Proton Synchrotron (SPS), and the Low-Energy Antiproton Ring (LEAR)] can provide sources of $p\bar{p}$ interactions which have unique characteristics. The internal gas target in ring 2 of the ISR[1-5] was successfully used in test periods, first with a coasting proton beam (October 1982 and March 1983) and then with an antiproton beam (May and July-August 1983). The internal target for the SPS[6] has been installed in the machine, and tests are in preparation.

The main problem created by the use of an internal gas target in a storage ring is the effect of the target gas on the coasting beam lifetime and characteristics (e.g. size, momentum). The most efficient solution to this problem is to apply horizontal and vertical betatron stochastic cooling and momentum stochastic cooling[7]. Also of great interest is the electron cooling foreseen in LEAR, which will extend the antiproton momenta range for experiments.

The features of the system, a coasting antiproton beam interacting on a gas internal target, are the following:

i) it has high luminosity ($\geq 10^{31}\,cm^{-2} \cdot s^{-1}$);
ii) the interaction region has small dimensions (of the order of 1 cm^3 or less); this is fundamental in order to simplify the design of the experimental apparatus and to facilitate the analysis of the experimental data;
iii) the value of the momentum resolution $\Delta p/p$ for the cooled antiproton beam is not spoiled by the interactions in the gas target;
iv) operation is continuous;
v) there is efficient use of antiprotons;
vi) there is a possibility of polarizing the atomic gas jet target;
vii) the effect of multiple scattering on the target is negligible for very low energy recoil protons or secondary particles.

The target which gives the largest luminosity is a type of molecular beam[8] called a 'cluster' beam, which provides a flow of gas at supersonic speed (hence the name of gas 'jet' target) due to the expansion of gas from a vessel at high pressure and low temperature into the vacuum through an injector (nozzle) of very small aperture (10-150 μm) and special geometry. The flow of gas is directional in the axis of the expansion and it is absorbed after having traversed the storage ring vacuum pipe (Fig. 1).

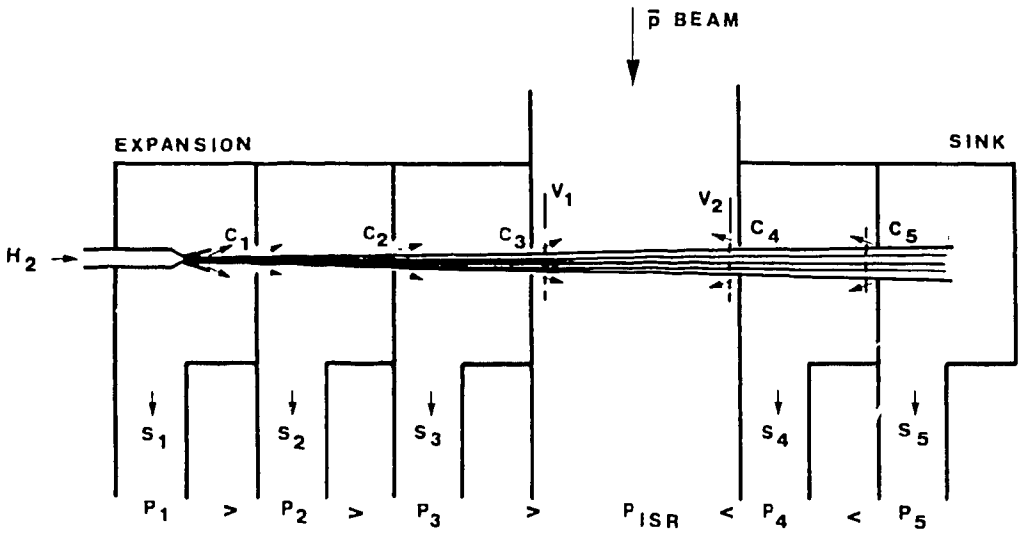

Stage	S	C
1	7000 ℓ/s	0.7 ℓ/s
2	4000 ℓ/s	3.0 ℓ/s
3	4000 ℓ/s	7.0 ℓ/s
ISR	2000 ℓ/s	80.0 ℓ/s
4	8000 ℓ/s	1100.0 ℓ/s
5	120000 ℓ/s	

Fig. 1 Scheme of the use of molecular beam as an internal gas target. $s_{1,5}$ and s_{ISR} are the speeds of the pumping systems acting on the different chambers and $p_{1,5}$ and p_{ISR} the respective pressures.

Section 2 describes the operations of molecular and atomic beams. Section 3 deals with the problems of the use of a jet target in a storage ring. To outline problems and solutions, I will describe many of the characteristics of the jet target of the ISR and that of the SPS.

2. MOLECULAR AND POLARIZED ATOMIC BEAMS

2.1 Effusive gas source

The simplest source one can consider is the effusive source. Gas at temperature T_0 and pressure p_0 is kept in vessel A (Fig. 2), which has a small hole with diameter d allowing the gas to flow towards vessel B ($p_B \ll p_A$). This establishes molecular flow conditions. Molecules in the forward direction can be selected with a screen between vessels B and C. The luminosity possible from this source is very low. For example: using H_2 in a source with $T_0 = 100$ K, $p_0 = 1$ Torr, $d = 50$ μm, $\lambda = 25.0$ μm, we obtain a gas flux with intensity $I(\theta) = 2.5 \times 10^{17} \times \cos\theta$ atoms per steradian per second. The luminosity of the interaction of a beam of 3×10^{11} antiprotons, coasting at a frequency of 3.3×10^5 Hz on an internal target built from this gas source, will be $\sim 2.5 \times 10^{26}$ $cm^{-2} \cdot s^{-1}$ taking into account the dimensions of the antiproton beam at the crossing with the H_2 beam (the H_2 beam diameter at the crossing point with the antiproton beam is ~ 1 cm at a distance of 26 cm from the H_2 beam origin).

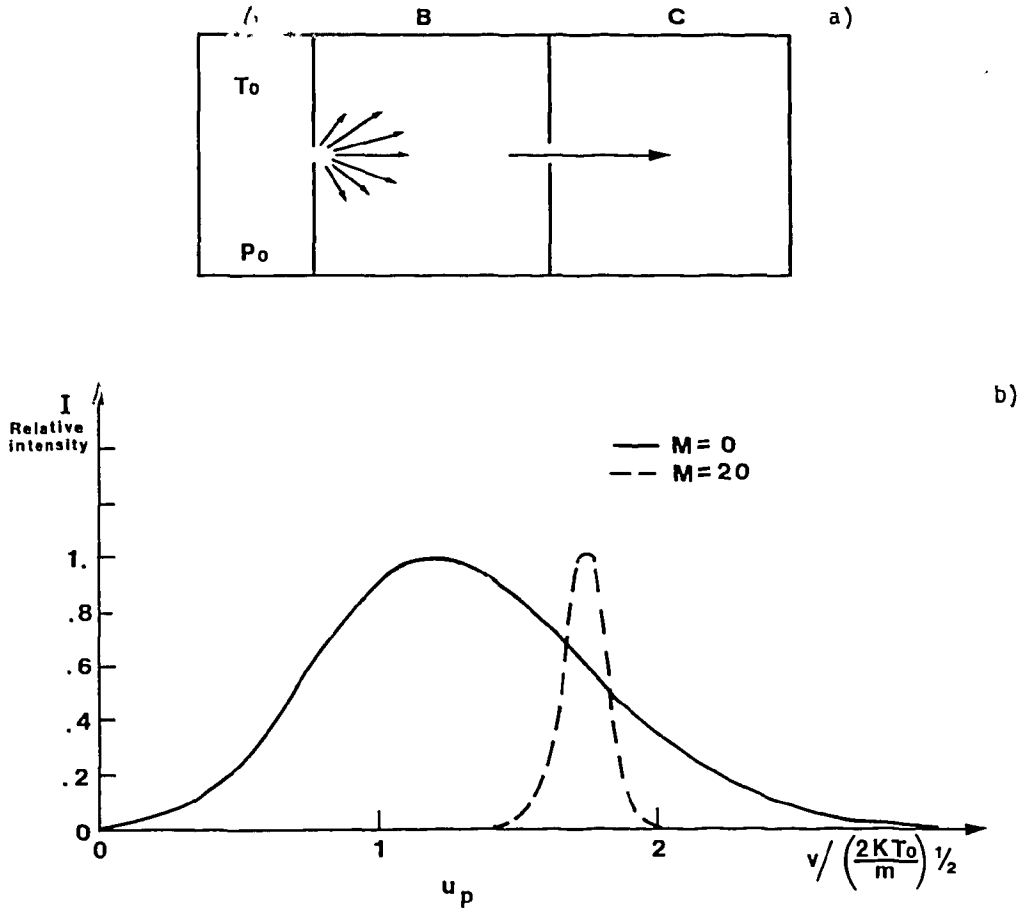

Fig. 2 Effusive gas source scheme and velocity distribution of molecules.

2.2 Sonic gas source

To increase the density of the gas source we have to consider the free expansion under continuum conditions. The gain with respect to the effusive source is that the final flow will be molecular, but the pressure (hence the density in the jet) can be increased in the initial state. In this case the gas in vessel A can escape to vessel B via an injector (nozzle) of the type shown in Fig. 3a. The equations that describe the expansion of the gas are derived from those for the conservation of energy and mass of a fluid flow: if we use the Mach number they can be expressed as[8]:

$$T = T_0\left[1 + (\alpha-1)\left(\frac{M^2}{2}\right)\right]^{-1} \tag{1}$$

$$p = p_0\left[1 + (\alpha-1)\left(\frac{M^2}{2}\right)\right]^{-\alpha/(\alpha-1)} \tag{2}$$

$$u = u_0 M\left[1 + (\alpha-1)\left(\frac{M^2}{2}\right)\right]^{-\frac{1}{2}} \tag{3}$$

$$n = n_0\left[1 + (\alpha-1)\left(\frac{M^2}{2}\right)\right]^{-1/(\alpha-1)} \tag{4}$$

$$A = \left(\frac{\alpha+1}{2}\right)^{-B}\left[1 + (\alpha-1)\left(\frac{M^2}{2}\right)\right]^{B}\left(\frac{A_0}{M}\right) \tag{5}$$

where

$B = (\alpha+1)/[2(\alpha-1)]$

u = local flow velocity

$\alpha = C_p/C_v$

A_0 = area of the cross-section of the nozzle throat

u_0 = velocity of molecules in the initial state

n_0 = density of molecules in the initial state .

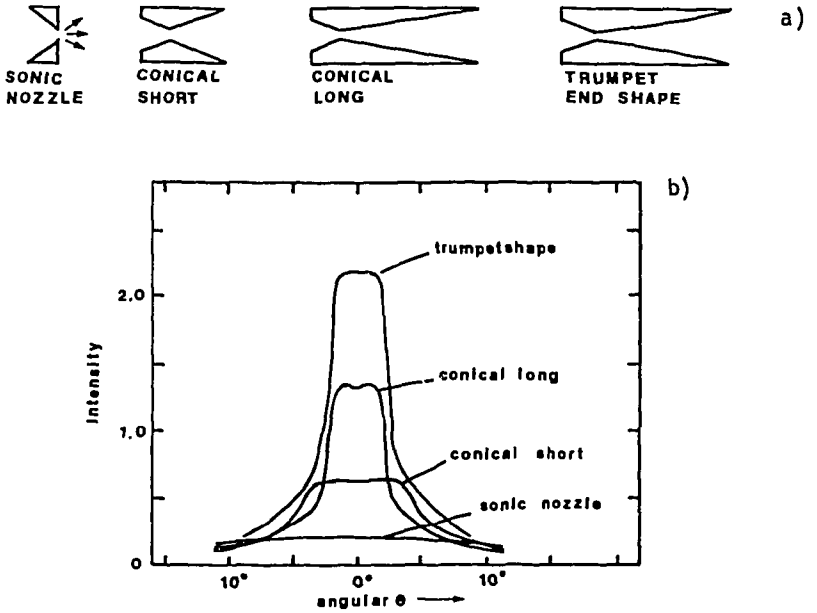

Fig. 3 a) Various types of nozzles. b) Mass flux distribution for nozzles with the same throat diameter and different geometries. For all distributions the stagnation condition and thus the nozzle mass flux are the same. The intensity scale is in units of 10^{22} atoms per steradian per second. (From Ref. 9.)

The nozzle flow field is similar to that from a point source close to the nozzle throat. At a short distance x from the nozzle throat, the streamlines are almost straight, the density decreases as $1/x^2$, and the flow velocity has approached its final value

$$v_{max} = u_0\left(\frac{\alpha-1}{2}\right)^{-0.5} . \tag{6}$$

We note that the velocity distribution (see Fig. 2b) has completely narrowed approaching the end of expansion. As for the effusive source we can fix the parameter for the gas source and

calculate the luminosity of interactions of an antiproton beam with an internal target built from this gas source. Suppose we can use $\Delta\Omega = 1.2 \times 10^{-3}$ sr of solid angle and a total flow I from the nozzle of 13 $cm^3 \cdot s^{-1} \approx 10$ Torr $\cdot \ell \cdot s^{-1}$. We get $I_0 = I\Delta\Omega = 4.2 \times 10^{17}$ molecules per second; the density expressed in molecules per cubic centimetre at the crossing point with the antiproton beam is given by

$$\rho = \frac{I_0}{A v_{max}} , \tag{7}$$

where A is the area of the cross-section of the gas flow at the crossing with the antiproton beam. For a 1 cm diameter beam with $v_{max} = 1290\ m \cdot s^{-1}$ we get a luminosity of $\sim 8 \times \times 10^{29}\ cm^{-2} \cdot s^{-1}$ if the beam intensity is 3×10^{11} antiprotons at a frequency of 3.3×10^5 Hz.

2.3 Cluster gas source

The use of a converging/diverging nozzle[9] increases the intensity in the axial direction of expansion of the gas by a large factor. Figure 3b displays the intensity of the gas source from different nozzles. All the nozzles have the same throat diameter, hence the same quantity of expanding gas. This is due to the fact that with a suitable geometry (Fig. 4a) of the nozzle (converging/diverging), the rate of expansion can be slowed down. Then the description of the expansion given above is only valid up to the cross-section of the diverging part of the nozzle, where the values of p and T of the expanding gas reach the corresponding vapour-pressure values (Fig. 4a). At this time the gas is saturated and as the expansion

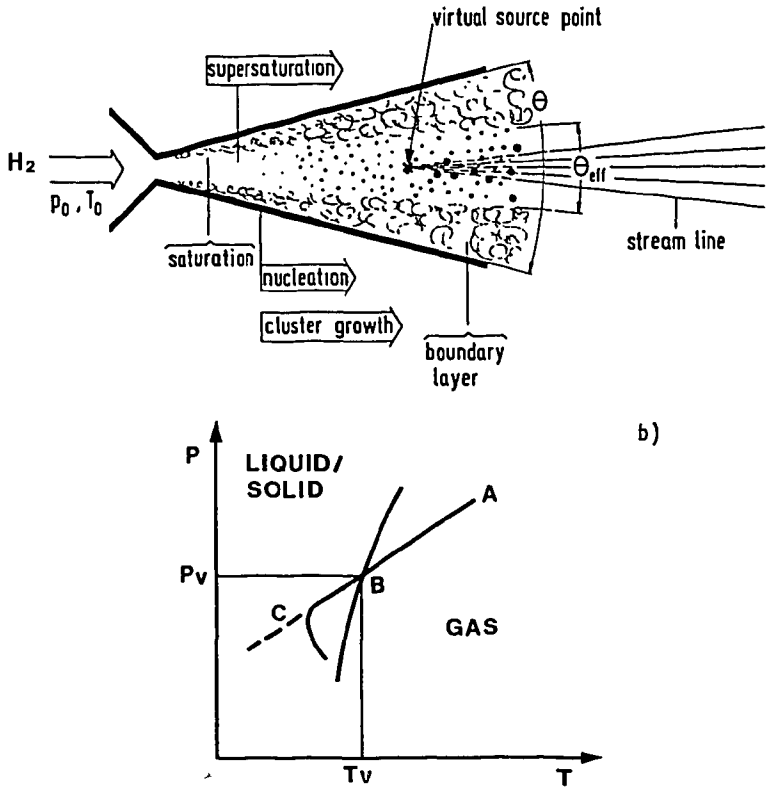

Fig. 4 a) Converging/diverging nozzles; the relevant phases of the generation of the gas beam are indicated. (From Ref. 9.) b) log p, log T diagram for H_2. p_v: vapour pressure. T_v: vapour temperature (see text).

goes on it will undergo a supersaturation condition in which, if the density and the pressure are large enough -- or in other words if the number of collisions is large -- the molecules start to form clusters. This nucleation phase will result in a central part of the beam being composed of clusters of molecules of a size which, depending on p_0, T_0, and nozzle geometry, can reach 10^5-10^6 molecules per cluster.

Figure 4b shows schematically the diagram of the expansion in a log p, log T plot. Expansion from point A to point B is described by Eqs. (1) to (5). The gas becomes supersaturated from B to C, and in C the formation and growth of clusters begin, that is to say p and T tend to move towards the equilibrium curve. The effects which are relevant for our applications are the following:

i) there is a formation of clusters;
ii) there is an increase in the density of the central region;
iii) clusters can fly straight for long distances in high-vacuum regions without disturbance from the residual gas.

A complete theory of condensation in beams of clusters has still not been formulated. The understanding of the thermodynamic properties of small clusters and the kinetics by which they are formed and destroyed is not complete. A complete condensation theory should be able to:

i) find the equilibrium concentration for a given cluster size in a supersaturated state;
ii) calculate the nucleation rate;
iii) calculate the further growth of clusters.

The main difficulties come from the fact that given a cluster size N, these clusters will not only interact with monomers but also with other clusters of any size.

A phenomenological approach is to try to formulate models which can find, from the properties of the beams of different gases, scaling laws which correlate the effects of initial pressure and temperature and the nozzle geometry. Let us consider as an example the corresponding jet model[8]. The main result of this model is to find the reduced values of p_0 and T_0 such that, on the assumption that the basic process (interaction of a cluster with a monomer) has the same strength for both gases, the properties of the beam of gas type 1 are the same as those of the beam of gas type 2.

$$p_0 = \frac{p_{0,1}}{\varepsilon_1/\sigma_1^3} = \frac{p_{0,2}}{\varepsilon_2/\sigma_2^3} = \text{const} \tag{8}$$

$$T_0 = \frac{T_{0,1}}{\varepsilon_1/K_1} = \frac{T_{0,2}}{\varepsilon_2/K_2} = \text{const}\,, \tag{9}$$

where for gas i,

ε_i: characteristic energy

σ_i: characteristic length

K_i: Knudsen number of expansion.

This is most valid for rare gases, but is also a good approximation for other gases (CO_2, N_2, etc). For the H_2 cluster beam a large effort has been devoted to formulating, from extensive measurements with different nozzle parameters[9], scaling laws for cluster size and intensity.

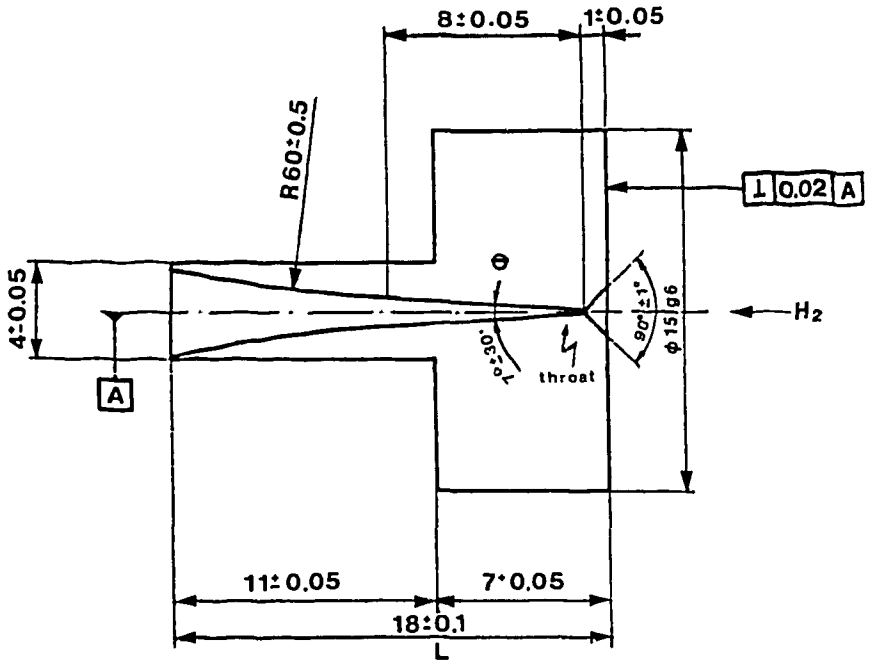

Fig. 5 Converging/diverging nozzle with special trumpet-shaped end part.

If the characteristics of the nozzle (Fig. 5) are semi-aperture θ, throat diameter D, length of diverging part L, one finds[9] that the cluster size N is

$$N \propto p_0 T_0^{-2.4} \left(\frac{D}{\operatorname{tg}\theta}\right)^{1.5} L^{0.2} , \tag{10}$$

with p_0 in pascals, T_0 in kelvins, and D and L in millimetres. The following observations are important:

i) N is limited: in fact p_0 and T_0 should be on the gaseous side of the vapour-pressure curve (Fig. 4b): at fixed T_0, p_0 cannot be raised above $p_V(T_0)$; and at fixed p_0, T_0 cannot be lowered below $T_V(p_0)$.

ii) The gas flux from the throat is $\propto p_0 d^2$: so a smaller nozzle throat implies a smaller gas flux for the same stagnation pressure p_0.

iii) The pressure in the expansion chamber should be < 10^{-1} Torr to avoid beam attenuation, thus implying that a powerful pumping system has to be employed for the expansion chamber.

The scaling law (10) can be applied if the characteristics of the injector are also scaled. For example, to get the same intensity from two nozzles, one with D_1 and θ_1, the other with D_2 and θ_2, we should use pressures $p_{0,1}$ and $p_{0,2}$ such that:

$$p_{0,1}\left(\frac{D_1}{\operatorname{tg}\theta_1}\right)^{1.5} = p_{0,2}\left(\frac{D_2}{\operatorname{tg}\theta_2}\right)^{1.5} . \tag{11}$$

For example, if $D_2 = D_1/3$ and $\theta_1 = 5°$, $\theta_2 = 3.5°$ we should use a pressure $p_{0,2} = 3p_{0,1}$. But the injector geometry to get the same expansion parameters is also different in the two cases and it should be calculated, according to Ref. 8, as follows:

$$\left(\frac{D_2}{2} + \ell \text{ tg } \theta_2\right)^2 = \left(\frac{D^2}{2}\right)^2 \left(\frac{\alpha+1}{2}\right)^{-B} \frac{\left[1 + (\alpha-1)(M^2/2)\right]^B}{M} , \qquad (12)$$

where ℓ is the distance from the nozzle throat and $B = (\alpha+1)/[2(\alpha-1)]$. The length L_2 of the nozzle is:

$$L_2 = \frac{D_2 \text{ tg } \theta_1 \, L_1}{D_1 \text{ tg } \theta_2} . \qquad (13)$$

The choice of the jet beam that can be used as the internal target in a storage ring depends on many parameters. The basic parameter is the luminosity of the interactions of the coasting beam on the jet target. It is expressed as:

$$L = I\omega\rho \ (\text{cm}^{-2} \cdot \text{s}^{-1}) , \qquad (14)$$

where

I: number of circulating antiprotons,
ω: their frequency of revolution,
ρ: density of the target (atoms per square centimetre).

The maximum luminosity is obtained for the largest value of ρ such that the beam lifetime and size and the momentum spread $\Delta p/p$ at equilibrium are still compatible with useful running conditions (a few days per antiproton injection). Fixing the density we can choose the other characteristics of the target, namely:

i) the geometry of the pumping systems to absorb the jet (to be built in such a way that apart from the gas in the jet, no other large gas quantity enters the vacuum pipe),
ii) the geometry of the production system,
iii) the distance from the nozzle throat to the interaction region, and the collimation geometry which determines the jet dimensions at the interaction region.

In the case of the ISR, we fixed the diameter of the H_2 beam at the crossing point with $\bar{p}$ = = 10 mm to match the particle beam equilibrium dimensions. The jet density had to be $\rho = 10^{14}$ atoms per square centimetre to obtain a luminosity of 10^{31} cm$^{-2} \cdot$ s^{-1} with 3×10^{11} antiprotons at 3.3×10^5 Hz. To determine the actual values of the jet parameters p_0, T_0, D, and the consequent nozzle geometry, the velocity of the clusters had to be fixed. Since we were working at $T_0 = 77$ K (liquid N_2 temperature) then $v_{max} = 1290$ m $\cdot$ s^{-1}. The jet intensity was $I \simeq 5 \times 10^{18}$ molecules per square centimetre per second $\simeq 4.4 \times 10^{21}$ molecules per steradian per second. This could be obtained with $p_0 \simeq 10^6$ Pa and a trumpet-shaped nozzle (Fig. 5) with the following characteristics: D = 30 μm, $\theta = 3.5°$, and L = 18 mm.

2.4 Polarized target

Atomic beams which can be obtained with the technique described above can be polarized with the selection of pure spin states[6,10]. In this case the formation of clusters has to be avoided and the resulting intensity will depend on i) the maximum pressure that can be used in the stagnation region without recombination (biatomic gas), ii) the value of T_0 of the source, and iii) the geometrical acceptance of the six-pole magnets used to focus the atoms in the interaction region. The speed of the atoms, which is a function of T_0, will influence the geometrical acceptance of the six-pole magnets. Polarized target of this type can reach densities of the order of 10^{11}-10^{12} atoms per square centimetre in the interaction region.

Stable atomic hydrogen can be produced at very low temperatures (0.3 K or below) with the use of very high fields (5-10 T) and all surfaces coated with a superfluid ^{4}He film[10]. An internal jet target could be built starting with a source of this type, but the technology is still in a development phase.

3. GASEOUS TARGETS IN STORAGE RINGS

3.1 Introduction

One of the characteristics of jet molecular or atomic beams is to be able to fly over long distances in high vacuum without absorption or diffusion by the rest gas. This, together with their high intensities, makes their use very attractive as internal targets. The problems are the following:

i) blow-up of the coasting beam dimensions and momentum degradation of the beam,
ii) increase of the pressure in the vacuum pipe of the ring.

These problems influence the lifetime of the beam and the luminosity that can be integrated for physics data taking. Other problems are connected with the operation of the target itself. Possible nozzle blockage or the contamination of the vacuum of the storage ring by the target system could lead to interruption of the operation for repairs, leading to loss of the coasting beam.

3.2 Target-system configuration

Figure 1 shows the schematic organization of an internal target. The jet of gas is produced in the gas expansion which takes place in chamber 1, and is absorbed in chamber 5 after having passed through chamber 2, chamber 3, the interaction region with the circulating particles, and chamber 4.

Our aim is to keep the value of the pressure in the interaction region (p_{int}) as near as possible to that in the case of operation of the storage ring without target. The clusters of the jet can enter and leave the vacuum pipe of the storage ring without perturbation of the pressure condition if the aperture towards the beam sink is large enough. So they will not produce a pressure rise in the interaction region. A rise of the pressure in the interaction region will only be provoked by the gas diffused in that region if $p_3 > p_{int}$ and $p_4 > p_{int}$. The amount of gas entering the storage ring vacuum pipe is $\dot{Q} = (P_3C_3 + P_4C_4)$, where C_3 and C_4 are the conductances between chambers 3 and 4 and the ISR vacuum pipe (see Fig. 1). And if $C_3 + C_4 \ll s_I$, where s_I is the pumping speed applied to the interaction region, we obtain $p_{int} = \dot{Q}/s_I$. Since C_3 and C_4 cannot be reduced below the values corresponding to the aperture needed to get the correct target dimensions at the interaction region with the circulating beam, one has to minimize p_3 and p_4, and maximize s_I; hence, the interest of interposing the maximum number of differential pumping stages compatible with the geometry of the system, in order to minimize the quantity of gas diffusing in the vacuum pipe. The reduction in pressure from chamber i to chamber i+1 is given by $p_{i+1}/p_i \simeq C_{(i\to i+1)}/s_{(i+1)}$ if $C_{(i\to i+1)} \ll s_{(i+1)}$.

3.3 Interactions of stored beam on the jet target

Losses of particles of the coasting beam can be caused by small-angle scattering, which adds up at each crossing. This multiple scattering blow-up can be compensated by a cooling

system which achieves transverse cooling time smaller than the multiple scattering blow-up time. Then particles of the beam are lost if they undergo (i) elastic scattering at angles larger than the machine acceptance or (ii) inelastic reactions.

$$I = I_0 \, e^{-\sigma\rho\omega t} \, , \tag{15}$$

where

I_0: initial intensity
ω : revolution frequency
ρ : density of the jet (atoms/cm^2),

$$\sigma = \sigma_{el}(> \theta_0) + \sigma_{inel} \tag{16}$$

θ_0 being the storage-ring acceptance angle.

3.4 Beam blow-up

The blow-up rate is

$$\frac{1}{\sigma}\frac{d\sigma}{dt} = 0.698 \, \frac{\bar{\beta} p_{ms}}{p^2 E} \, , \quad E = (\alpha^2-1)^{-\frac{1}{2}}\varepsilon \, , \tag{17}$$

where

$\alpha = \frac{1}{2}\left[(E\bar{\beta})/\pi\right]^{\frac{1}{2}}$,

p_{ms} = equivalent distributed N_2 pressure.

To counteract multiple scattering the cooling rate should be of the order of or larger than the blow-up rate.

The beam size at equilibrium is found from the emittance balance. If E_{ms} is the rate of emittance increase due to the multiple scattering and E_c is the rate of emittance due to cooling, then (in real life corrections have to be applied to take into account electronic noise):

$$\frac{dE}{dt} = \dot{E}_{ms} + \dot{E}_c \tag{18}$$

$$\dot{E}_{ms} = 0.4(\beta)^{3/2} \, \frac{p_{ms}}{p^2} \tag{19}$$

$$\dot{E}_c = \frac{2}{\tau} E \tag{20}$$

where τ is the amplitude cooling time

$$E(t) = \left(1 - e^{-2t/\tau}\right)\tau \, \frac{\dot{E}_{ms}}{2} + E_0 \, e^{-2t/\tau} \, , \tag{21}$$

where E_0 is the initial beam emittance.

3.5 Beam loss by target system breakdown

Nozzle blockage can occur owing to mechanical blockage (remember the nozzle throat is very small) or condensation of gas on the cold nozzle. The pumping systems should be oil-free and fast acting ultra-high vacuum (UHV) valves should separate the target system from the vacuum pipe to avoid contamination or sudden pressure bump.

3.6 ISR internal target

The density of the target[11] was chosen as the maximum compatible with a reasonable beam lifetime, and the beam characteristics were determined by the horizontal and vertical cooling systems of the ISR[7]. The gas jet dimensions were determined by a series of skimmers, which also separate the production system into three different stages. Each stage had an individual 'oil-free' pumping system. The nozzle was mounted on a moving mechanism to optimize its position with respect to the axis defined by the skimmers and thus the intensity. The jet was absorbed in the sink system, which was built of three cryogenic pumps dimensioned to minimize the flow of gas streaming back towards the interaction region (Figs. 6, 7).

A system to monitor the jet intensity was mounted before the last cryopump, which was very large (120,000 $\ell \cdot s^{-1}$). The monitor gives a measurement of the vertical projection of the jet intensity. The dimensions of the interaction region were 6 × 8 × 10 mm^3. This is very helpful in the design of a compact experimental apparatus and enhances its capability Also, analysis of data is easier (pattern recognition, etc.).

Particular care was devoted to the H_2 injection line in order to avoid nozzle blockages by gas impurities. The following points are very important:

i) the use of pure H_2 (10 ppm maximum),
ii) the use of mechanical filters (2 μm),
iii) the use of a condensation trap (LN_2 temperature),
iv) the use of an active charcoal trap (LN_2 temperature).

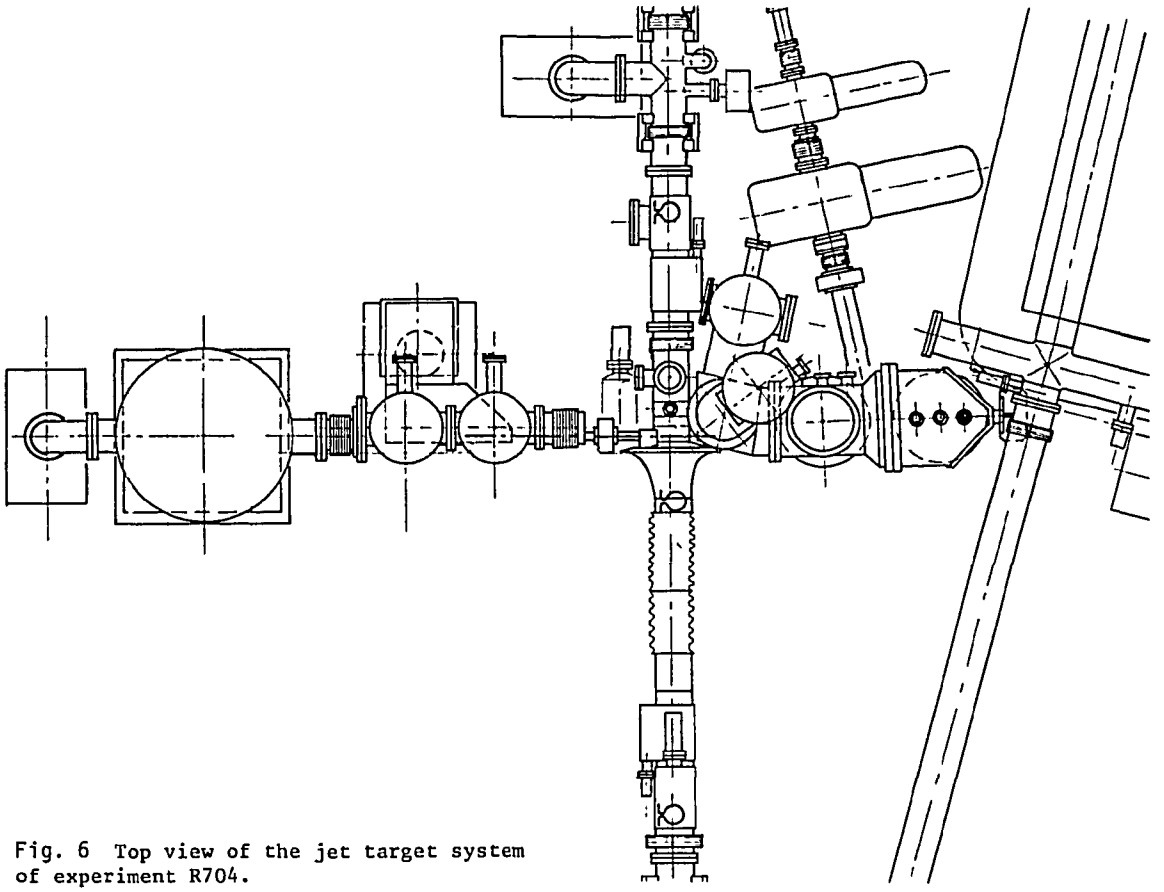

Fig. 6 Top view of the jet target system of experiment R704.

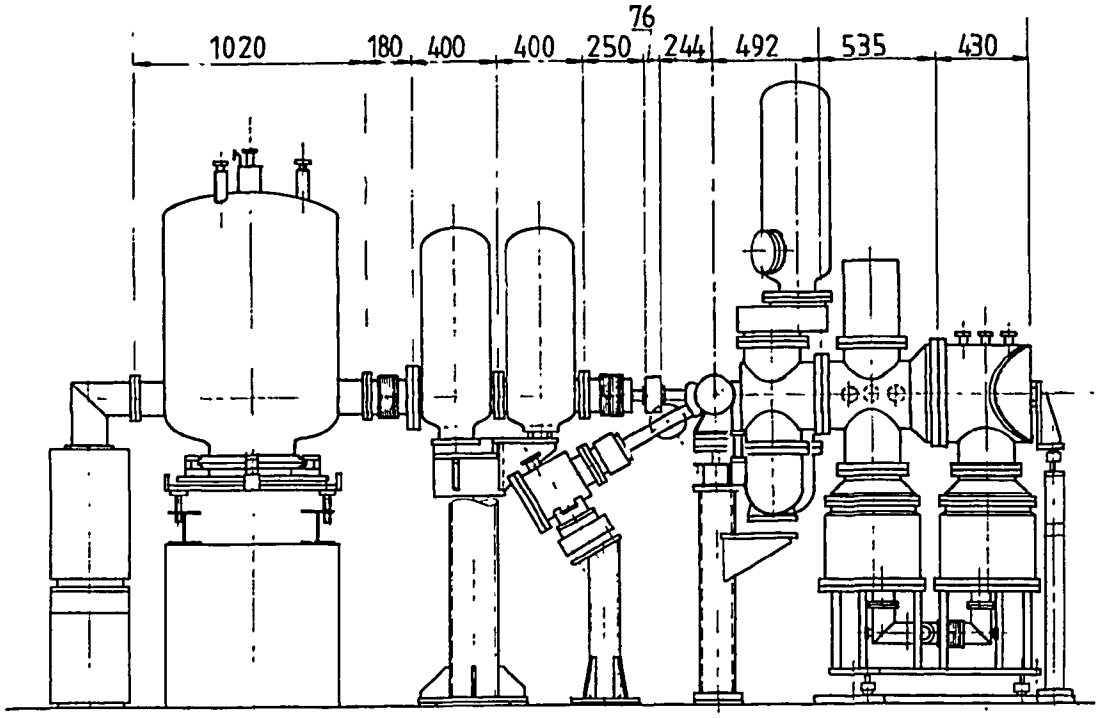

Fig. 7 Side view of the jet target system of experiment R704.

3.6.1 Ease of on/off jet conditions

Two UHV valves separated the production and sink from the vacuum pipe. This was to prevent the possible contamination of ISR ring 2 in the case of a large pressure bump due to breakdown in the target system.

3.6.2 Beam lifetime and loss rate

The loss rate is a function of the target thickness, rest gas, machine aperture, and stochastic cooling performances.

The amount of H_2 seen by the coasting antiproton beam was

i) rest gas around the ISR ($p = 10^{-11}$ Torr) $\approx 10^{-12}$ g · cm^{-2}
ii) gas diffused around the jet $\sim 2 \times 10^{-12}$ g · cm^{-2}
iii) gas in the target $\sim 1.5 \times 10^{-10}$ g · cm^{-2}.

Then most of the gas was in the target. The experience of all runs in the ISR with an internal target was that horizontal and vertical stochastic cooling worked well. The vertical cooling completely nullified the blow-up caused by the target. Loss rate at a maximum target density was $\sim$ 170 ppm, i.e. the beam had a lifetime of 100 h. This value is for the worst case when p = 3.68 GeV/c and it is near to that obtained from the total $p\bar{p}$ nuclear cross-section alone.

3.6.3 Momentum resolution

The horizontal cooling system in the ISR was very effective in reducing the $\Delta p/p$ of the beam, in order to stabilize the central value of the momentum. This was also the case with the jet on (Fig. 8).

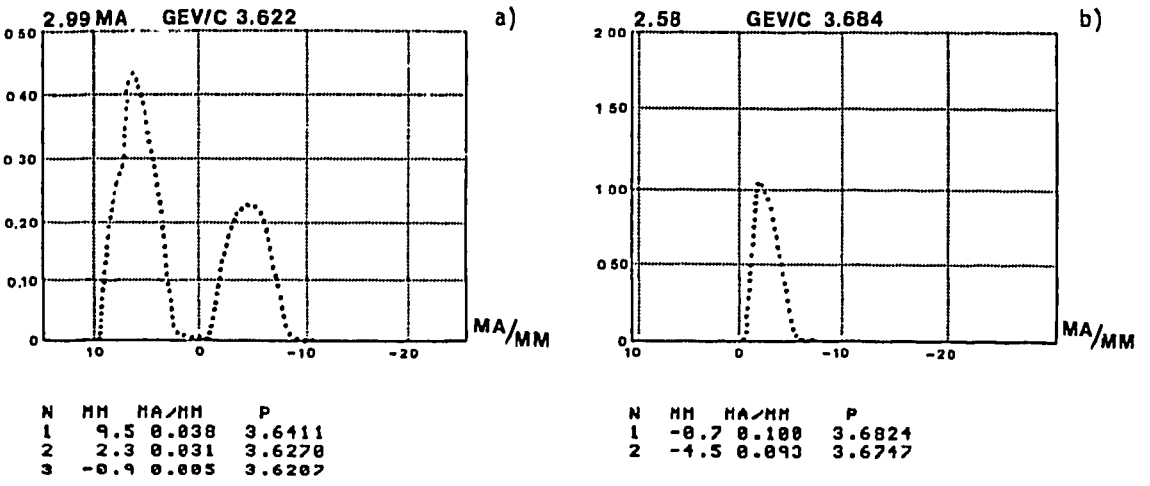

Fig. 8 a) Two pulses stacked in run 1366 during initial momentum cooling. b) Final stack after 12 hours of physics and continued momentum cooling. (Note change of vertical scale.)

The value of $\Delta p/p$ can be as low as 4×10^{-4} when the antiprotons traverse the jet target. In this case, in 'formation' experiments the width of the state will be measured using the machine parameters rather than the resolution given by the experimental apparatus. This leads to a much better precision of the measurement, for example:

$$\Delta M \simeq \frac{0.938}{\sqrt{s}} \Delta p \ , \quad \Delta M(\eta_c) = 460 \text{ keV} \ . \tag{22}$$

Final-state particles had to traverse a thickness of 0.3 mm of stainless steel. This does not introduce a large multiple scattering angle. If the detection takes place inside the vacuum pipe, particles of very low momentum can be detected: the luminosity monitor is, for example, obtained through the measurement of recoil protons of momentum. It should be mentioned here that there have been applications of an internal target in Saturn at Saclay[12] (Fig. 9) and at FLAB[13] to measure pp elastic scattering at very small angles. This last application is only suitable for an accelerating cycle.

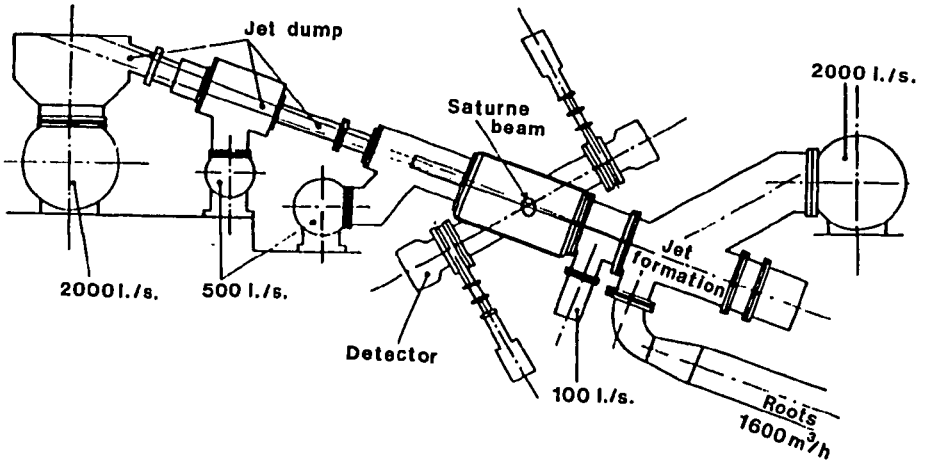

Fig. 9 Saclay jet target system.

3.7 SPS jet target

The working conditions are T_0 = 30 K, $p_0 = 1 \times 10^5$ Pa. The nozzle is trumpet-shaped with a throat diameter of 100 μm (Figs. 10 and 11). The thickness is 4×10^{14} atoms per square centimetre, in order to compensate for the reduced revolution frequency. With 6×10^{11} anti-protons in the coating beam the luminosity is

$$L = 10^{31}\ \mathrm{cm}^{-2} \cdot \mathrm{s}^{-1}\ . \qquad (23)$$

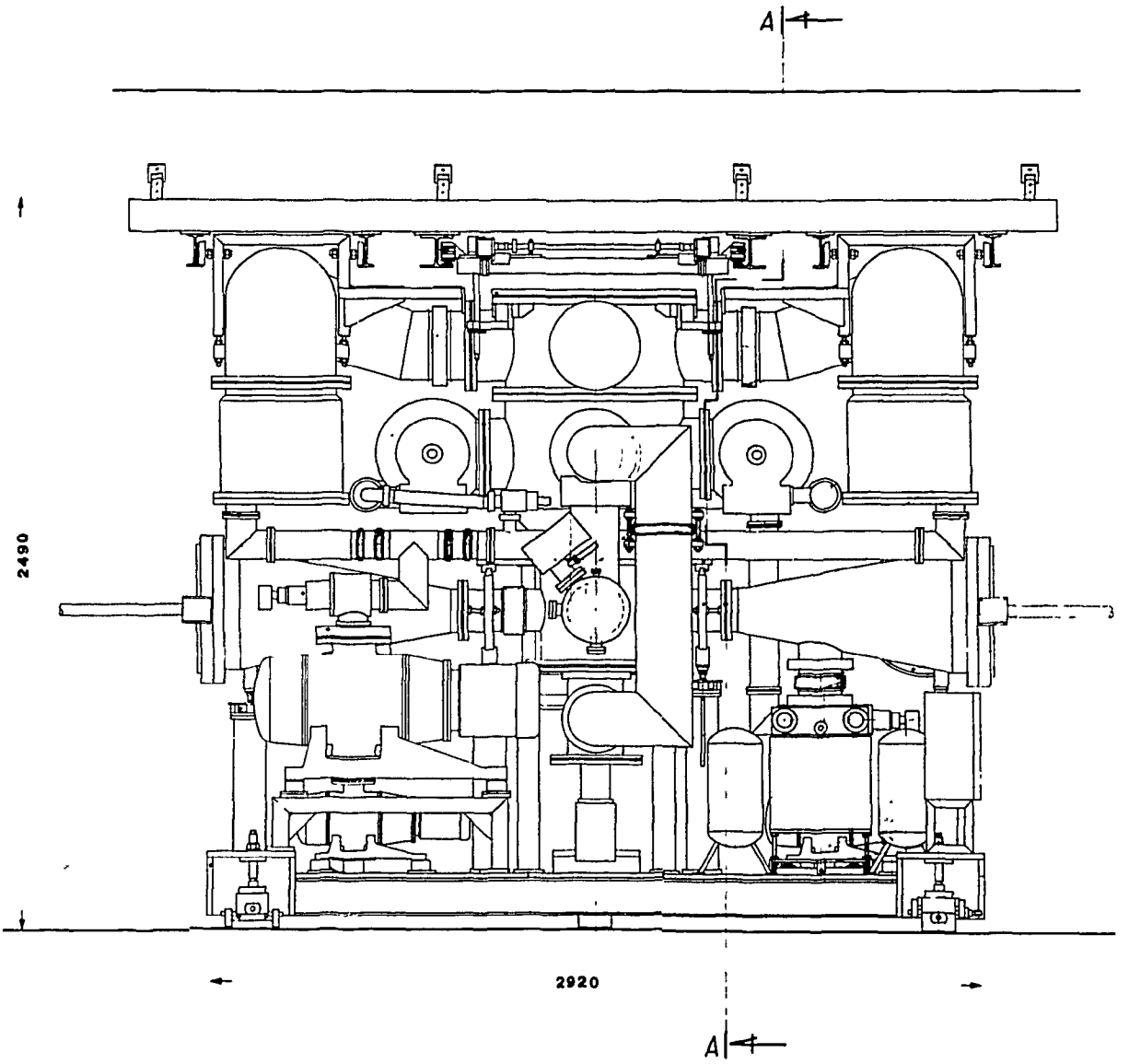

Fig. 10 SPS jet target system.

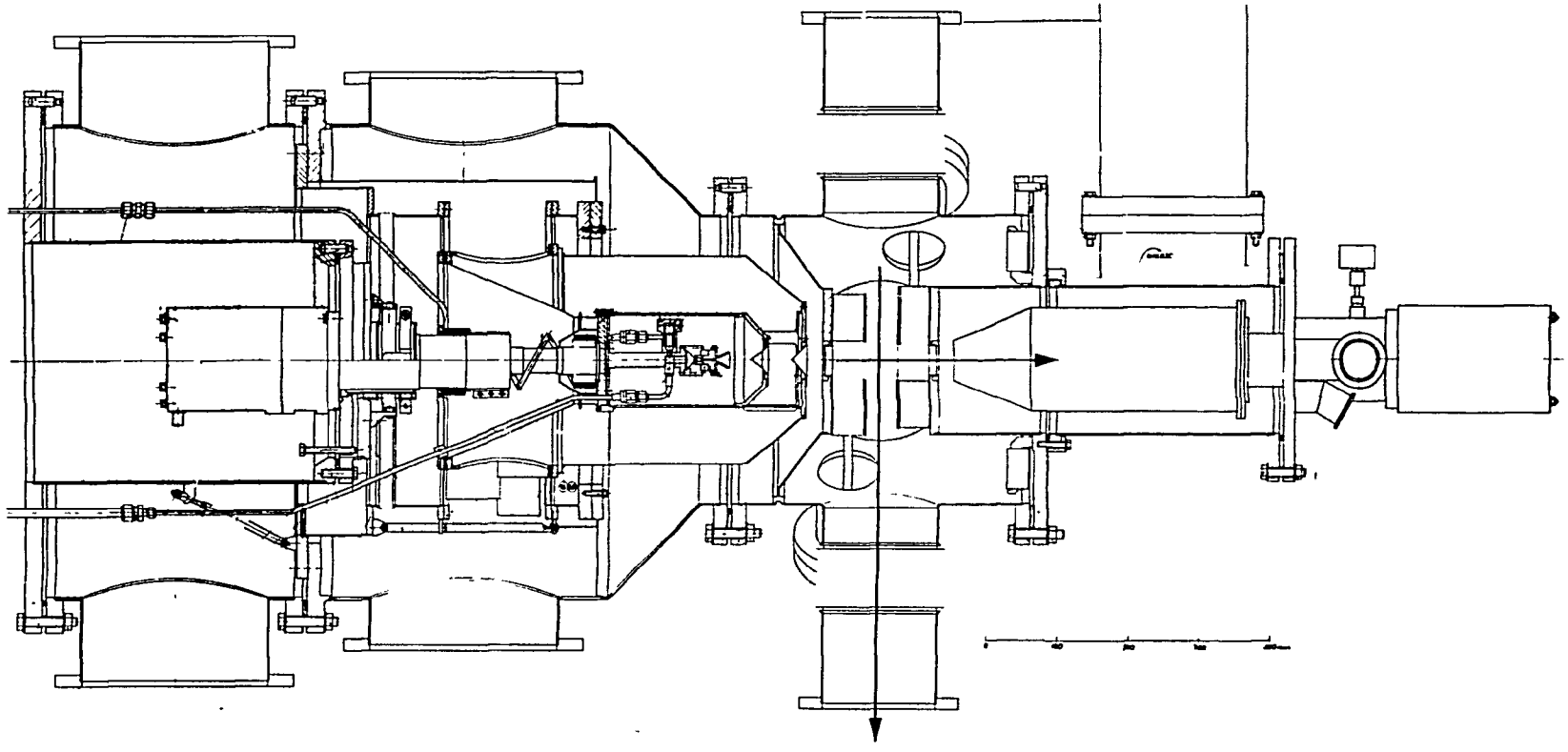

Fig. 11 SPS jet target system with details of expansion-chamber arrangement.

This is a compromise in order to reduce the $p\bar{p}$ Collider luminosity by 10% per day. In this case the momentum of the beam is 270 GeV/c.

The multiple-scattering contribution to beam blow-up is less important, but no stochastic cooling is applied. The calculated losses are 3% per day. The calculated losses due to interaction luminosity (both beams are affected) are 6% per day. Tests are in preparation.

Also of great importance is the test to measure the perturbation induced by the target on the UA1 and UA2 experiments. In fact this target operation is foreseen together with the UA1 and UA2 experiments (parasitic operations).

3.8 A jet target for LEAR

The third possible use is in LEAR[14]. The problems are much the same as in the ISR, but the momenta range is in lower values (0.1-2 GeV/c). The following conditions are needed:

- stochastic cooling (this exists);
- electron cooling, which would reduce the $\Delta p/p$ and enlarge the range of momenta for a jet operation (this is envisaged);
- low-β insertion at the beam-jet crossing to increase the machine acceptance (this would reduce loss by multiple scattering).

Depending on the beam momentum various modes of operation can be foreseen. A thickness of the target as large as 10^{14} atoms per square centimetre can be obtained and used. The actual thickness will depend on beam momentum, availability of antiprotons from the Antiproton Accumulator (AA), and the intensity of pulse transferred from it[14]. This would provide a very powerful tool to perform experiments which would benefit from the performances of the antiproton beam interacting on an internal gas target that I have been discussing.

4. CONCLUSION

The availability of a molecular cluster jet beam opens up new possibilities in high-energy physics experiments. This is particularly true in the case of experiments performed with cooled antiproton beams.

The source of $p\bar{p}$ interactions provided by the coasting antiproton beam (to which cooling) is applied) hitting a jet target provides a very efficient tool to study in detail the annihilation processes leading to the formation of narrow resonant states, and could be the experimental tool to establish the existence of glueballs, Higgs, and exotic states.

Acknowledgements

I wish to express my warm thanks to Professor U. Valbusa for the helpful conversations I have had with him.

REFERENCES

1) C. Baglin et al., Charmonium spectroscopy at the ISR using an antiproton beam and a hydrogen jet target, CERN/ISRC/80-14 (1980).

2) C. Baglin et al., First evidence of J/ψ formation in antiproton-proton annihilation, *in* Proc. 1983 Int. Symposium on Lepton and Photon Interactions at High Energies, Cornell, 1983 (Cornell University, Ithaca, 1983), p. 906.

3) R. Cester, Formation of charmonium states in antiproton-proton annihilation, *in* Proc. Workshop on Heavy Flavours, Como, 1983 (Ed. Frontières, Paris, 1984) p. 327.

4) C. Baglin et al., Antiproton collisions with a gas H_2 jet and formation of charmonium states, *in* Proc. 12th Int. Conf. on High Energy Accelerators, Fermilab, Batavia, 1983 (Fermilab, Batavia, 1984), p. 251.

5) ISR performance report, CERN/LEP-ISR-OP/64 (1983).

6) J. Antille et al., CERN/SPSC/80-63 (1980).

7) D. Möhl, lecture at this School.
C. Taylor, lecture at this School.
A. Peschard and M. Studer, Stochastic cooling in the CERN ISR during $p\bar{p}$ colliding beam physics, CERN/LEP/ISR/RF/83-15 (1983).

8) O.F. Hagena and W. Obert, Cluster formation in expanding supersonic jets, J. Chem. Phys. 56, 1793 (1972).
O.F. Hagena, Surface Science, 106, 101 (1981).

9) W. Obert, Properties of clusters beams formed with supersonic nozzles, 11th Symposium on Rarefied Gas Dynamics, Cannes, 1978 (CEA, Paris, 1978), p. 1181.

10) T.O. Niinikoski, CERN-EP/83-124 (1983) and references therein.

11) M. Macri, A clustered H_2 beam, *in* Physics with Low Energy Cooled Antiprotons (Plenum, New York, 1983) p. 432.

12) R. Burgel et al., Nucl. Instrum. Methods 204, 53 (1982).

13) V.A. Nikitin et al., Adventures in Experimental Physics 8, 263 (1972).

14) LEAR Design Study, CERN/PS/DL/80-7 (1980).
P. Lefevre, D. Möhl and G. Plass, *in* Proc. 11th Int. Conf. on High Energy Accelerators, Geneva, 1980 (Birkhäuser, Basel, 1980), p. 819.
K. Kilian and D. Möhl, CERN $\bar{p}$ LEAR note 44 (1979).